J Fluoresc (2014) 24:1537–1544
DOI 10.1007/s10895-014-1442-8

ORIGINAL PAPER

Design and Synthesis of a New Terbium Complex-Based Luminescent Probe for Time-Resolved Luminescence Sensing of Zinc Ions

Zhiqiang Ye · Yunna Xiao · Bo Song · Jingli Yuan

Received: 3 June 2014 / Accepted: 20 August 2014 / Published online: 30 August 2014

Abstract Luminescent probes/chemosensors based on lanthanide complexes have shown great potentials in various bioassays due to their unique long-lived luminescence property for eliminating short-lived autofluorescence with time-resolved detection mode. In this work, we designed and synthesized a new dual-chelating ligand {4′-[*N*,*N*-bis(2-picolyl)amino]methylene-2,2′:6′,2′-terpyridine-6,6′-diyl} bis(methylenenitrilo) tetrakis(acetic acid) (BPTTA), and investigated the performance of its Tb^{3+} complex (BPTTA-Tb^{3+}) for the time-resolved luminescence sensing of Zn^{2+} ions in aqueous media. Weakly luminescent BPTTA-Tb^{3+} can rapidly react with Zn^{2+} ions to display remarkable luminescence enhancement with high sensitivity and selectivity, and such luminescence response can be realized repeatedly. Laudably, the dose-dependent luminescence enhancement shows a good linear response to the concentration of Zn^{2+} ions with a detection limit of 4.1 nM. To examine the utility of the new probe for detecting intracellular Zn^{2+} ions, the performance of BPTTA-Tb^{3+} in the time-resolved luminescence imaging of Zn^{2+} ions in living HeLa cells was investigated. The results demonstrated the applicability of BPTTA-Tb^{3+} as a probe for the time-resolved luminescence sensing of intracellular Zn^{2+} ions.

Keywords Terbium complex · Luminescent probe · Zinc ions · Time-resolved luminescence sensing

Z. Ye · Y. Xiao · B. Song · J. Yuan (✉)
State Key Laboratory of Fine Chemicals, School of Chemistry, Dalian University of Technology, Dalian 116024, People's Republic of China
e-mail: jlyuan@dlut.edu.cn

Introduction

Due to the important physiological functions of Zn^{2+} ions in human body, the researches on the Zn^{2+}-involved bioprocesses as well as the relative Zn^{2+} detection techniques have attracted much attention in the past years [1–4]. In biosystems, although most of Zn^{2+} ions are tightly bound to various metallo-proteins, the labile pools of Zn^{2+} ions are presented in many tissues such as brain, intestine, pancreas, and retina [5]. The disruption of Zn^{2+} homeostasis has been known to be implicated in health disorders including Alzheimer's disease [5–7] and diabetes [8]. For the real-time monitoring of Zn^{2+} ions in biosystems, especially those in living cells, the luminescent imaging technique using Zn^{2+}-responsive luminescence probes and an appropriate imaging instrument is one of the most promising methods due to its high spatial and temporal resolution capacities, and for this purpose, a variety of organic dye-based fluorescence probes for Zn^{2+} ions, such as the derivatives of fluorescein [9], rhodamine [10], dipyrroylmethane (BODIPY) [11] and cyanine [12], have been successfully developed and used for the monitoring of Zn^{2+} ions in various biosamples in recent years. However, for the bioimaging application, the organic dye-based fluorescence probes have several problems including the interference of autofluorescence from complicated biosamples, the photobleaching of organic dyes, and the measurement errors caused by the excitation and scattering lights due to the small Stokes shifts of organic dyes [13, 14].

Compared to fluorescent organic dyes, luminescent lanthanide (mainly Tb^{3+} and Eu^{3+}) complexes exhibit several unique luminescence properties, such as long luminescence lifetimes, large Stokes shifts and sharp emission profiles, which allow the complexes to be easily used as probes for the time-resolved luminescence measurement to eliminate the interferences of short-lived autofluorescence and scattering lights [15, 16]. In recent decades, several lanthanide complex-based luminescent probes for Zn^{2+} ions have been synthesized [17,

18], but the bioimaging application of these probes suffers from the problems of their insufficient sensitivity and selectivity, and rather short excitation wavelength (~260 nm). Recently, we also synthesized a Tb^{3+} complex-based luminescent probe for Zn^{2+} ions, {2,6-bis(3′-aminomethyl-1′-pyrazolyl)-4- [N,N-bis(2-picolyl)amino-methylenepyridine]} tetrakis(acetate)-Tb^{3+} (BBATA-Tb^{3+}), and demonstrated its applicability for the time-resolved luminescence imaging of intracellular Zn^{2+} ions [19]. The main drawbacks of BBATA-Tb^{3+} as a luminescent probe for Zn^{2+} ions are its lower ability to distinguish Zn^{2+} from Cd^{2+} (its luminescence response to Cd^{2+} ions is ~90 % corresponding to that to Zn^{2+} ions) as well as the shorter excitation wavelength (318 nm).

To improve the properties of the Tb^{3+} complex-based luminescent probe for Zn^{2+} ions, in this work, we further designed and synthesized a new dual-chelating ligand that can simultaneously coordinate with Tb^{3+} and Zn^{2+} in aqueous buffers, {4′-[*N,N*-bis(2-picolyl)amino]methylene- 2,2′:6′,2′-terpyridine-6,6′-diyl}bis(methylenenitrilo) tetrakis(acetic acid) (BPTTA), and systematically investigated the luminescence response behavior of its Tb^{3+} complex to Zn^{2+} ions. In this ligand, the terpyridine polyacid moiety was used as a light-absorption-antenna instead of 2,6-bis(N-pyrazolyl)pyridine polyacid moiety in BBATA for sensitizing the Tb^{3+} luminescence because its coordination ability to Tb^{3+} is stronger and the excitation wavelength of its Tb^{3+} complex is longer (330–335 nm) [20–22], and the bis(2-picolyl)amino moiety was still used as a Zn^{2+} recognition moiety since it can play two roles to modulate the Tb^{3+} luminescence: quenching the excited state of the antenna via a photo-induced electron transfer (PET) process to switch-off the Tb^{3+} luminescence in the absence of Zn^{2+} ions, and coordinating with Zn^{2+} to switch-on the Tb^{3+} luminescence in the presence of Zn^{2+} ions [19].

To evaluate the utility of BPTTA-Tb^{3+} for imaging the intracellular Zn^{2+} ions, the acetoxymethyl ester of BPTTA (AM-BPTTA) was synthesized since it can be easily transferred into the living cells together with Tb^{3+} ions by the ordinary incubation method, and in the cells, the rapid generation of BPTTA-Tb^{3+} accompanied by the hydrolysis of acetoxymethyl ester catalyzed by ubiquitous intracellular esterases [23, 24] enables the Zn^{2+} ions to be imaged. The luminescence imaging results demonstrated the applicability of BPTTA-Tb^{3+} as a new luminescent probe for the sensing of intracellular Zn^{2+} ions. Scheme 1 shows the structure of BPTTA-Tb^{3+} and its luminescence response reaction to Zn^{2+} ions.

Experimental

Materials and Physics Measurements

Tetraethyl (4′-bromomethyl-2,2′:6′,2′-terpyridine-6,6′-diyl) bis(methylenenitrilo) tetrakis(acetate) (compound 1) was synthesized according to the previous method [25]. Tetrahydrofuran (THF) and acetonitrile were used after appropriate distillation and purification. HeLa cells were obtained from Dalian Medical University. Unless otherwise specified, all chemical materials were purchased from commercial sources and used without further purification.

^{1}H and ^{13}C NMR spectra were recorded on a Bruker Avance spectrometer (400 MHz for ^{1}H and 100 MHz for ^{13}C). Mass spectra were measured on a HP1100LC/MSD electrospray ionization mass spectrometer (ESI-MS). Elemental analysis was carried out on a Vario-EL CHN analyzer. Time-resolved luminescence spectra were measured on a Perkin-Elmer LS 50B luminescence spectrometer with the settings of excitation wavelength, 332 nm; emission wavelength, 540 nm; delay time, 0.2 ms; gate time, 0.4 ms; cycle time, 20 ms; excitation slit, 10 nm; and emission slit, 5 nm. Luminescence quantum yields of the Tb^{3+} complexes were measured by using the previous method [20, 21]. The calibration curve (Fig. 4B) for the time-resolved luminescence detection of Zn^{2+} ions using BPTTA-Tb^{3+} as a probe in a 96-well microtiter plate was measured on a Perkin-Elmer Victor 1420 multilabel counter with the settings of excitation wavelength, 330 nm; emission wavelength, 540 nm; delay time, 0.2 ms; counting time, 0.4 ms; and cycling time, 1.0 ms. All bright-field, steady-state luminescence and time-resolved luminescence imaging measurements were carried out on a laboratory-use luminescence microscope [26].

Synthesis of the Ligand BPTTA

The reaction pathway for the synthesis of the new ligand BPTTA is shown in Scheme 2. For the synthesis of compound 2, a mixture of compound 1 (0.34 g, 0.47 mmol), K_2CO_3 (0.66 g, 4.7 mmol) and di(2-picolyl)amine (0.11 g, 0.56 mmol) in 20 mL of dry acetonitrile was stirred at room temperature for 24 h under an argon atmosphere. After filtration, the solvent was evaporated, and the residue was purified by silica gel column chromatography using CH_2Cl_2-CH_3OH (20:1, v/v) as eluent. The compound 2, tetraethyl {4′-[N,N-bis(2-picolyl)amino]methylene-2,2′:6′,2′- terpyridine-6,6′-diyl} bis(methylenenitrilo) tetrakis(acetate), was obtained as yellow oil (0.20 g, 51 % yield). ^{1}H NMR ($CDCl_3$): δ=1.23 (t, *J*= 7.2 Hz, 12H), 3.72 (s, 8H), 3.92 (s, 4H), 4.01 (s, 4H), 4.14 (q, *J*=7.2 Hz, 8H), 4.22 (s, 2H), 7.15-7.19 (m, 2H), 7.35 (d, *J*= 8.0 Hz, 2H), 7.63-7.66 (m, 2H), 7.76 (d, *J*=8.0 Hz, 2H), 7.83 (t, *J*=8.0 Hz, 2H), 8.49 (d, *J*=8.0 Hz, 2H), 8.55 (d, *J*=8.0 Hz, 2H), 8.58 (s, 2H). ^{13}C NMR ($CDCl_3$): δ=14.2, 54.4, 54.9, 57.8, 60.1, 60.5, 119.6, 120.7, 122.1, 123.0, 136.7, 137.5, 148.9, 149.3, 155.4, 155.6, 158.3, 158.9, 159.3, 171.2. ESI-MS (*m/z*): calcd. for $C_{46}H_{54}N_8O_8$, 846.4; found, 847.5 ($[M + H]^+$).

For the synthesis of BPTTA, a mixture of compound 2 (0.20 g, 0.24 mmol), KOH (0.44 g, 7.87 mmol), 0.88 mL H_2O and 12 mL ethanol was stirred at room temperature for 20 h.

Scheme 1 Structure of BPTTA-Tb^{3+} and its luminescence response reaction towards Zn^{2+} ions (the photos show the luminescence colors of solutions of the two complexes under a 365 nm UV lamp)

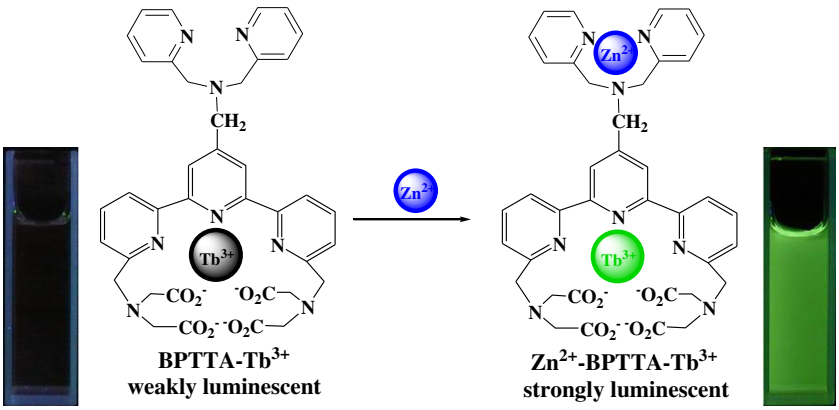

After evaporation, the residue was dissolved in 1.5 mL of water, and pH of the solution was adjusted to ~3 with HCl (3 M). To the solution was added 50 mL of acetone, and the precipitate was collected by filtration and washed by acetone. After drying, the precipitate was extracted 5 times by boiling acetonitrile (5×50 mL). Combination and evaporation of the filtrates gave the target product as a brown solid (75 mg, 42.5 % yield). ^{1}H NMR (DMSO-d_6): δ=3.86 (s, 8H), 4.22 (s, 4H), 4.37 (s, 4H), 4.40 (s, 2H), 7.56-7.58 (m, 2H), 7.66 (d, J=8.0 Hz, 2H), 7.86-7.90 (m, 2H), 8.03 (t, J=8.0 Hz, 2H), 8.10 (t, J=8.0 Hz, 2H), 8.50 (s, 2H), 8.51 (d, J=8.0 Hz, 2H), 8.70 (d, J=8.0 Hz, 2H). ^{13}C NMR (DMSO-d_6): δ=55.0, 58.0, 59.3, 65.5, 120.4, 121.7, 124.6, 125.6, 139.0, 141.5, 146.1, 149.1, 152.3, 154.5, 155.0, 155.6, 156.5, 171.6. ESI-MS (m/z): calcd. for $C_{38}H_{38}N_8O_8$, 734.2; found, 735.3 ([M + H]$^+$). Elemental analysis calcd. (%) for $C_{38}H_{38}N_8O_8 \cdot 3H_2O$ (BPTTA·$3H_2O$): C 57.86, H 5.62, N 14.21; found (%): C 57.55, H 5.82, N 14.58.

Synthesis of the Complex BPTTA-Tb^{3+}

BPTTA (19.7 mg, 0.025 mmol) and $TbCl_3 \cdot 6H_2O$ (9.3 mg, 0.025 mmol) were added into 5.0 mL of 0.1 M Tris–HCl buffer of pH 7.2. After the mixture was stirred at room temperature for 0.5 h, the obtained stock solution (5.0 mM) of BPTTA-Tb^{3+} was stored at −20 °C, and suitably diluted with aqueous buffers before use.

Luminescence Titration of BPTTA-Tb^{3+} with Zn^{2+} Ions

All the experiments were carried out in 0.1 M Tris–HCl buffer of pH 7.2 at room temperature. After different concentrations of Zn^{2+} ions were added into the BPTTA-Tb^{3+} solution (5.0 μM), respectively, the solutions were stirred for 15 min at room temperature, and then subjected to the time-resolved luminescence measurement on the Perkin-Elmer LS 50B luminescence spectrometer. For the calibration curve measurement, the solutions of BPTTA-Tb^{3+} (0.1 μM) reacted with different concentrations of Zn^{2+} ions (0.0 – 1.0 μM) were added into the wells of a 96-well microtiter plate (80 μL per well), and then the plate was subjected to the time-resolved luminescence measurement on the Perkin-Elmer Victor 1420 multilabel counter.

Reactions of BPTTA-Tb^{3+} with Various Metal ions

All the reactions were carried out in 0.1 M Tris–HCl buffer of pH 7.2 at room temperature. After the BPTTA-Tb^{3+} solution (5.0 μM) was reacted with 2.0 equiv. of different metal ions (Na^+, K^+, Mg^{2+}, Ca^{2+}, Ba^{2+}, Pb^{2+}, Mn^{2+}, Fe^{2+}, Fe^{3+}, Co^{2+}, Ni^{2+}, Cu^{2+}, Ag^+, Zn^{2+}, Cd^{2+}) for 15 min, respectively, the emission intensities of the solutions at 540 nm were measured on the Perkin-Elmer LS 50B luminescence spectrometer.

Scheme 2 Reaction pathway for the synthesis of BPTTA

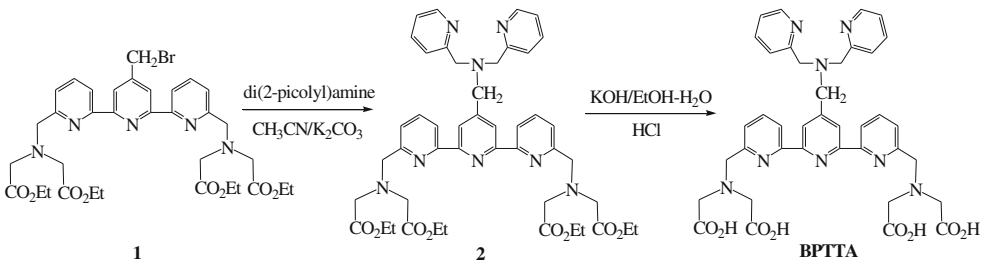

Luminescence Imaging of Intracellular Zn^{2+} Ions Using BPTTA-Tb^{3+} as a Probe

The stock solution (~50 mM) of AM-BPTTA was prepared by reacting BPTTA (6.3 mg, 8.0 μmol) with bromomethyl acetate (31 μL, 320 μmol) in anhydrous DMSO (117 μL) in the presence of triethylamine (12 μL, 80 μmol) for 48 h at room temperature. Before the solution was used for cell loading, it was 200-fold diluted with the cell culture medium (RPMI-1640 medium, supplemented with 10 % fetal bovine serum, 1 % penicillin and 1 % streptomycin) containing 0.25 mM $TbCl_3$.

The BPTTA-Tb^{3+}-loaded HeLa cells were prepared by incubating the cells with 2.0 mL of the above culture medium in a 25 cm^2 glass culture bottle at 37 °C in a 5 % CO_2/95 % air incubator. After incubation for 2 h, the Tb^{3+} complex-loaded cells were washed three times with Krebs-Ringer phosphate buffer (KRP buffer: 114 mM NaCl, 4.6 mM KCl, 2.4 mM $MgSO_4$, 1.0 mM $CaCl_2$, 15 mM Na_2HPO_4/NaH_2PO_4, pH 7.4), and then the cells were further incubated with the KRP buffer containing 0.5 mM Zn^{2+} for 1 h at 37 °C in the incubator. The cells were washed three times with KRP buffer, and then subjected to the steady-state and time-resolved luminescence imaging measurements.

The microscope (TE2000-E, Nikon), equipped with a 100 W mercury lamp, a UV-2A filters (Nikon, excitation filter, 330–380 nm; dichroic mirror, 400 nm; emission filter, >420 nm) and a color CCD camera system (RET-2000R-F-CLR-12-C, Qimaging Ltd.) was used for the steady-state luminescence imaging measurement with an exposure time of 15 s. The microscope, equipped with a 30 W xenon flash lamp (Pulse 300, Photonic Research Systems Ltd.), a UV-2A filters, and a time-resolved digital black-and-white CCD camera system (Photonic Research Systems Ltd.), was used for the time-resolved luminescence imaging measurement with the conditions of delay time, 100 μs; gate time, 1 ms; lamp pulse width,6 μs; and exposure time, 180 s. The time-resolved luminescence images are shown in pseudo-color treated by a SimplePCI software [26].

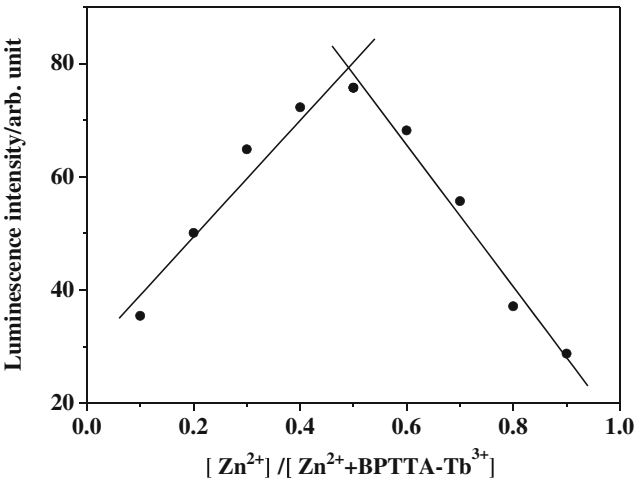

Fig. 2 Job's plot of the reaction between BPTTA-Tb^{3+} and Zn^{2+} in 0.05 M Tris–HCl buffer of pH 7.2. The total concentration of BPTTA-Tb^{3+} and Zn^{2+} was kept at 5.0 μM

Results and Discussion

Luminescence Properties of BPTTA-Tb^{3+} and Its Reaction Product with Zn^{2+} Ions

Figure 1 shows the time-resolved excitation and emission spectra of BPTTA-Tb^{3+} in the absence and presence of Zn^{2+} ions in 0.1 M Tris–HCl buffer of pH 7.2. The complex BPTTA-Tb^{3+} itself is weakly luminescent, exhibiting a maximum excitation peak at 332 nm ($\varepsilon_{332nm}=1.57\times10^4$ cm^{-1} M^{-1}) and a

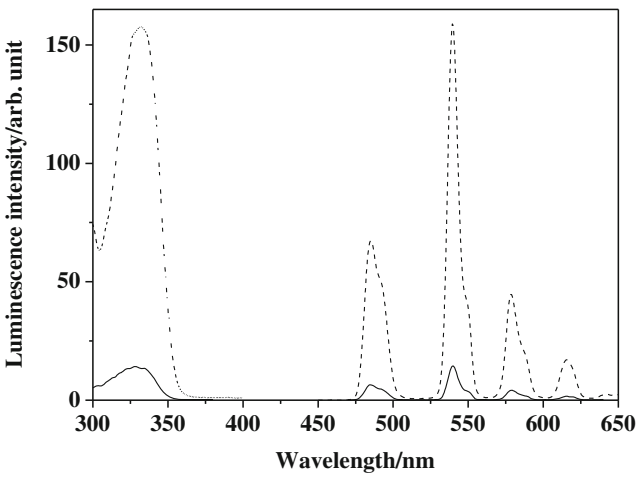

Fig. 1 Excitation (300–400 nm) and emission (450–650 nm) spectra of BPTTA-Tb^{3+} (5.0 μM) in the absence (solid lines) and presence (dashed lines) of Zn^{2+} ions (5.0 μM) in 0.1 M Tris–HCl buffer of pH 7.2

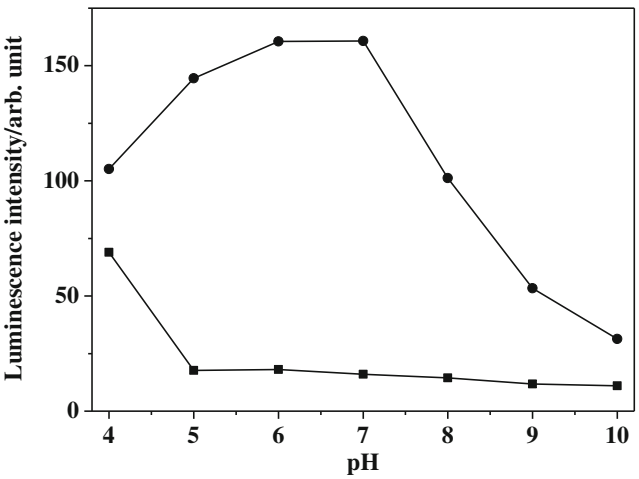

Fig. 3 Effects of pH on the emission intensities (540 nm) of BPTTA-Tb^{3+} (5.0 μM) and Zn^{2+}-BPTTA-Tb^{3+} (5.0 μM) in 0.1 M Tris–HCl buffers at different pH values

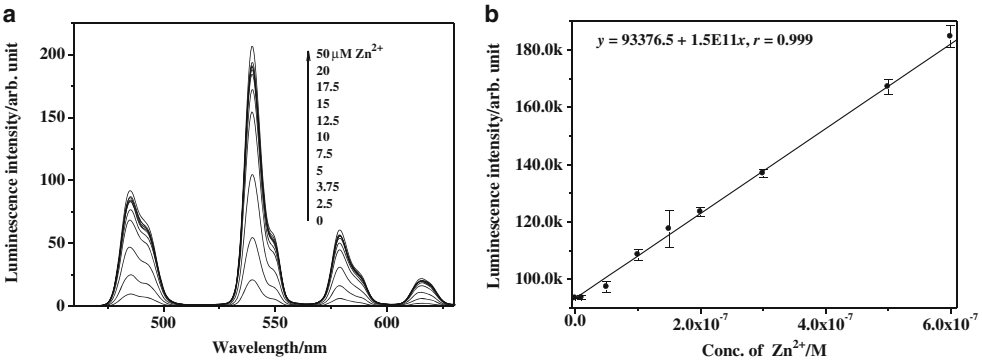

Fig. 4 a Time-resolved emission spectra (λ_{ex}=332 nm) of BPTTA-Tb^{3+} (5.0 μM) in the presence of different concentrations of Zn^{2+} in 0.1 M Tris–HCl buffer of pH 7.2. b Calibration curve for time-resolved luminescence detection of Zn^{2+} ions using BPTTA-Tb^{3+} (0.1 μM) as a probe in a 96-well microtiter plate

typical Tb^{3+} emission pattern with a main peak at 540 nm (φ< 0.5 %, τ=0.25 ms) and several side peaks centred at 485, 579, 616, and 643 nm, respectively. However, upon reaction with 1.0 equiv. of Zn^{2+} ions, the complex becomes strongly luminescent with an 11-fold luminescence enhancement and a remarkably prolonged luminescence lifetime (ε_{332nm}=1.89×10^4 cm^{-1} M^{-1}, φ=2.9 %, τ=1.13 ms). These results reveal that the bis(2-picolyl)amino moiety in BPTTA-Tb^{3+} can truly modulate the "off-on" luminescence behaviors of the Tb^{3+} complex through its coordination reaction with Zn^{2+} ions, which provides a clear signal for the luminescent sensing of Zn^{2+} ions in aqueous media.

To further confirm the coordination of the bis(2-picolyl)amino moiety in BPTTA-Tb^{3+} to Zn^{2+} ions, the reaction of BPTTA-Tb^{3+} with Zn^{2+} ions was investigated by the Job's plotting analysis method. As shown in Fig. 2, the Job's plot of the reaction between BPTTA-Tb^{3+} and Zn^{2+} exhibited a maximum at ~0.5 molecular fraction, which indicates that the bis(2-picolyl)amino moiety in BPTTA-Tb^{3+} can indeed coordinate to Zn^{2+} with a 1:1 stoichiometry, and such coordination reaction induces the luminescence enhancement of the solution.

The effects of pH on the emission intensities of BPTTA-Tb^{3+} and Zn^{2+}-BPTTA-Tb^{3+} were investigated in 0.1 M Tris–HCl buffers with different pH values ranging from 4.0 to 10.0. As shown in Fig. 3, the emission intensity of BPTTA-Tb^{3+} is weak and stable at pH>5.0 (luminescence increase of BPTTA-Tb^{3+} at pH<5 is due to the protonation of its bis(2-picolyl)amino moiety, which results in the PET efficiency decrease), while that of Zn^{2+}-BPTTA-Tb^{3+} is gradually increased with the pH increase in the range of pH 4.0–7.0, and significantly decreased with the pH increase in the range of pH 7.0–10.0. This phenomenon can be explained as follows: the pH-dependent luminescence increase of Zn^{2+}-BPTTA-Tb^{3+} in acidic pH range is due to the deprotonation of the bis(2-picolyl)amino moiety, which allows the moiety to coordinate to Zn^{2+} more easily, while the pH-dependent luminescence decrease of Zn^{2+}-BPTTA-Tb^{3+} in basic pH range is due to the hydrolysis of Zn^{2+} ions, which causes the dissociation of Zn^{2+}-BPTTA-Tb^{3+} by the formation of Zn(II) hydroxides. The above results suggest that the pH value around 7.0 could be optimal for the luminescence response of BPTTA-Tb^{3+} towards Zn^{2+} ions. Considering that BPTTA-Tb^{3+} was designed as a probe for sensing the intracellular Zu^{2+} ions, the buffer of pH 7.2 was used as the solvent for the characterization of the complex's luminescence properties in this work.

Luminescence Response of BPTTA-Tb^{3+} towards Zn^{2+} Ions

To quantitatively investigate the luminescence response behavior of BPTTA-Tb^{3+} to Zn^{2+} ions, the time-resolved emission spectra of BPTTA-Tb^{3+} (5.0 μM) upon reaction with different concentrations of Zn^{2+} ions were recorded in 0.1 M Tris–HCl buffer of pH 7.2. As shown in Fig. 4a, the emission intensities of BPTTA-Tb^{3+} at several emission wavelengths showed clearly pronounced increases with the increase of Zn^{2+} concentration. Furthermore, the dose-dependent luminescence enhancement at 540 nm followed a good linear relationship with the Zn^{2+} concentration in the range of 0.0~0.6 μM (Fig. 4b). The detection limit, calculated according to the reported method defined by IUPAC [27], is 4.1 nM, which indicates that BPTTA-Tb^{3+} can be used as a highly sensitive probe for the quantitative time-resolved luminescence detection of Zn^{2+} ions in aqueous media.

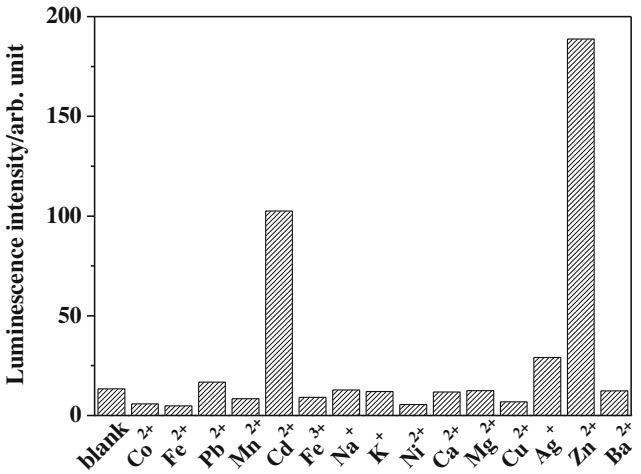

Fig. 5 Time-resolved emission intensities of BPTTA-Tb^{3+} (5.0 μM) at 540 nm in the absence and presence of various metal ions (10.0 μM)

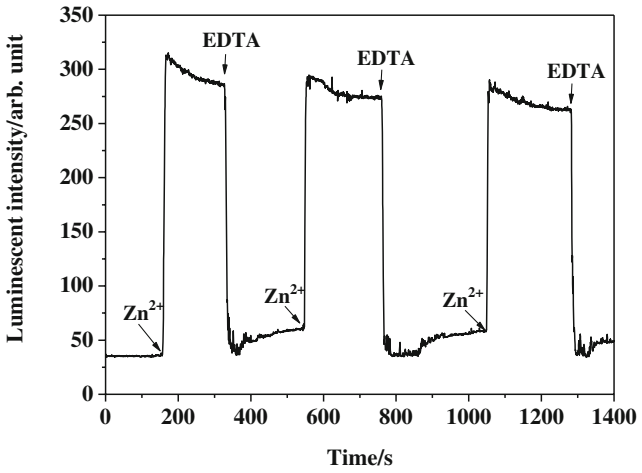

Fig. 6 Real-time luminescence responses of BPTTA-Tb^{3+} (10.0 μM) to the additions of Zn^{2+} (10.0 μM) and EDTA (10.0 μM) in 0.1 M Tris–HCl buffer of pH 7.2

To examine the luminescence response specificity of BPTTA-Tb^{3+} to Zn^{2+} ions, the time-resolved emission intensity changes of BPTTA-Tb^{3+} (5.0 μM) at 540 nm in the absence and presence of various metal ions (Na^{+}, K^{+}, Mg^{2+}, Ca^{2+}, Ba^{2+}, Pb^{2+}, Mn^{2+}, Fe^{2+}, Fe^{3+}, Co^{2+}, Ni^{2+}, Cu^{2+}, Ag^{+}, Zn^{2+}, Cd^{2+}, 10.0 μM) were recorded in 0.1 M Tris–HCl buffer of pH 7.2. As shown in Fig. 5, except for Zn^{2+} and Cd^{2+}, BPTTA-Tb^{3+} did not show significant luminescence responses to other metal ions including those that exist at much higher cellular concentrations, such as Na^{+}, K^{+}, Mg^{2+} and Ca^{2+} ions. Although the emission intensity of BPTTA-Tb^{3+} was also enhanced in the presence of Cd^{2+} ions, BPTTA-Tb^{3+} showed a better selectivity than the previous probe BBATA-Tb^{3+}. The luminescence response of BPTTA-Tb^{3+} to Cd^{2+} ions is ~54 % corresponding to that to Zn^{2+} ions. This result indicates that the specificity can be remarkably improved by using BPTTA-Tb^{3+} instead of BBATA-Tb^{3+} for the time-resolved luminescence detection of Zn^{2+} ions.

Furthermore, the temporal dynamics and reversibility of the luminescence response of BPTTA-Tb^{3+} to Zn^{2+} ions were examined by real-time recording the emission intensity changes of BPTTA-Tb^{3+} upon the repeat additions of Zn^{2+} ions and ethylenediamine tetraacetic acid (EDTA), respectively. As shown in Fig. 6, after the addition of Zn^{2+} ions, the emission intensity of BPTTA-Tb^{3+} was rapidly increased, and then kept at a high level for a long time under continuous excitation. When a stronger Zn^{2+}-chelator, EDTA, was added, the emission intensity was rapidly returned to the original level of free BPTTA-Tb^{3+}. Followed by the additions of Zn^{2+} and EDTA, respectively, the emission intensity of the solution displayed the reversible increase and decrease as the pulse responses. This result indicates that the luminescence response of BPTTA-Tb^{3+} to Zn^{2+} ions is very fast with good reversibility.

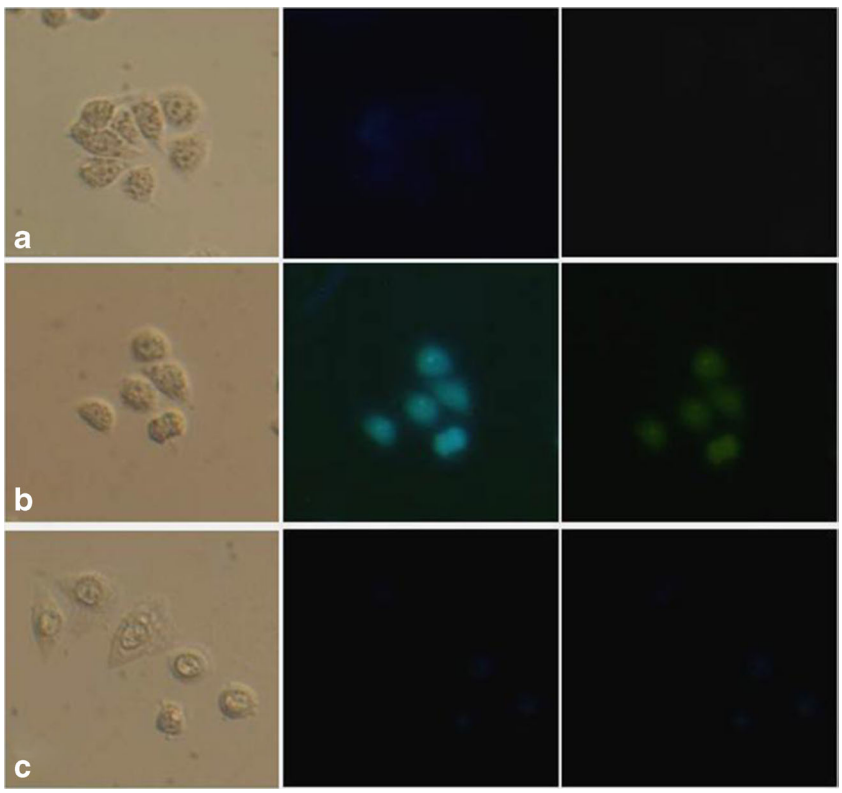

Fig. 7 Bright-field (*left*), steady-state luminescence (*middle*) and time-resolved luminescence (*right*) images of living HeLa cells at different incubation conditions. **a** The cells were incubated with 0.25 mM AM-PAMTTA-Tb^{3+} for 2 h; **b** the cells of (a) were further incubated with 0.5 mM Zn^{2+} for 1 h; **c** the cells of (b) were further incubated with 0.8 mM TPEN for 0.5 h

Luminescence Imaging of Intracellular Zn^{2+} Ions Using BPTTA-Tb^{3+} as a Probe

To evaluate the applicability of BPTTA-Tb^{3+} for the time-resolved luminescence imaging of Zn^{2+} ions in living cells, the BPTTA-Tb^{3+}-loaded HeLa cells were prepared by incubating the cells with the medium containing AM-BPTTA and Tb^{3+}. After the cells were incubated for 2 h, and further incubated with the Zn^{2+}-containing medium for 1 h, the bright-field, steady-state luminescence and time-resolved luminescence images of the cells were recorded.

As shown in Fig. 7, after incubation with the medium containing AM-BPTTA-Tb^{3+}, the cells showed only weak autofluorescence from cell components under the steady-state mode, and no luminescence signals could be observed under the time-resolved mode (Fig. 7a). However, followed the incubation of the cells with the Zn^{2+}-containing medium, bright cyan luminescence signals under the steady-state mode (mixture of blue and green emissions from cell components and the Tb^{3+} complex) and strong green luminescence signals under the time-resolved mode (from the Tb^{3+} complex) were clearly observed from the cells (Fig. 7b). These results indicate that BPTTA-Tb^{3+} can be used as a luminescence probe for the time-resolved luminescence imaging of intracellular Zn^{2+} ions without the interference of background fluorescence. To confirm the reversibility of the luminescence response of BPTTA-Tb^{3+} to intracellular Zn^{2+} ions, the Zn^{2+}-BPTTA-Tb^{3+}-loaded HeLa cells in Fig. 7b were further treated with *N,N,N',N'*-tetrakis(2-pyridyl)ethylenediamine (TPEN), a membrane-permeable Zn^{2+} chelator that can effectively remove Zn^{2+} ions, for another 30 min. In this case, both the steady-state and time-resolved luminescence signals of the HeLa cells were remarkably weakened (Fig. 7c), suggesting that BPTTA-Tb^{3+} could still act as a reversible luminescence probe for the monitoring of intracellular Zn^{2+} ions.

Conclusions

In summary, a new Tb^{3+} complex-based luminescence probe, BPTTA-Tb^{3+}, for the time-resolved luminescence sensing of Zn^{2+} ions in aqueous and cell samples has been synthesized and characterized in this work. Compared to the previously reported lanthanide complex-based luminescence probes for Zn^{2+} ions, BPTTA-Tb^{3+} showed the longer excitation wavelength and the better specificity to respond to Zn^{2+} ions. Taking advantages of high sensitivity and specificity, good water solubility and stability, and excellent photophysical properties of lanthanide complex probes, BPTTA-Tb^{3+} was successfully used for the time-resolved luminescence imaging of Zn^{2+} ion in living cells. The results demonstrated the applicability of the probe for the in vivo sensing of intracellular Zn^{2+} ions, which would be a useful tool for the luminescence monitoring of Zn^{2+} ions in complicated biosamples.

Acknowledgements Financial supports from the National Natural Science Foundation of China (Grant No. 21275025) and the Specialized Research Fund for the Doctoral Program of Higher Education of China (Grant No. 20130041130003) are gratefully acknowledged.

References

1. Frederickson CJ (1989) Neurobiology of zinc and zinc-containing neurons. Int Rev Neurobiol 31:145–238
2. Tomat E, Lippard SJ (2010) Imaging mobile zinc in biology. Curr Opin Chem Biol 14:225–230
3. Sasaki H, Hanaoka K, Urano Y, Terai T, Nagano T (2011) Design and synthesis of a novel fluorescence probe for Zn^{2+} based on the spirolactam ring-opening process of rhodamine derivatives. Bioorg Med Chem 19:1072–1078
4. Que EL, Domaille DW, Chang CJ (2008) Metals in neurobiology: probing their chemistry and biology with molecular imaging. Chem Rev 108:1517–1549
5. Bush AI, Pettingell WH, Multhaup G, Paradis M, Vonsattel JP, Gusella JF, Beyreuther K, Masters CL, Tanzi RE (1994) Rapid induction of Alzheimer a beta amyloid formation by zinc. Science 265:1464–1467
6. Bush AI (2003) The metallobiology of Alzheimer's disease. Trends Neurosci 26:207–214
7. Frederickson CJ, Koh JY, Bush AI (2005) The neurobiology of zinc in health and disease. Nat Rev Neurosci 6:449–462
8. Chausmer AB (1998) Zinc, insulin and diabetes. J Am Coll Nutr 17: 109–115
9. Hirano T, Kikuchi K, Kojima H, Urano Y, Higuchi T, Nagano T (2000) Highly zinc-selective fluorescent sensor molecules suitable for biological applications. J Am Chem Soc 122:12399–12400
10. Sensi SL, Ton-That D, Weiss JH, Royhe A, Gee KR (2003) A new mitochondrial fluorescent zinc sensor. Cell Calcium 34:281–284
11. Wu Y, Peng X, Guo B, Fan J, Zhang Z, Wang J, Cui A, Gao Y (2005) Boron dipyrromethene fluorophore based fluorescence sensor for the selective imaging of Zn^{2+} in living cells. Org Biomol Chem 3:1387–1392
12. Kiyose K, Kojima H, Urano Y, Nagano T (2006) Development of a ratiometric fluorescent zinc ion probe in near-infrared region, based on tricarbocyanine chromophore. J Am Chem Soc 128:6548–6549
13. Yang R, Li K, Liu F, Li N, Zhao F, Chan W (2003) 3,3′,5,5′-Tetramethyl-N-(9-anthrylmethyl) benzidine: a dual-signaling fluorescent reagent for optical sensing of aliphatic aldehydes. Anal Chem 75:3908–3914
14. Peng X, Song F, Lu E, Wang Y, Zhou W, Fan J, Gao Y (2005) Heptamethine cyanine dyes with a large stokes shift and strong fluorescence: a paradigm for excited-state intramolecular charge transfer. J Am Chem Soc 127:4170–4171
15. Yuan J, Wang G (2005) Lanthanide complex-based fluorescence label for time-resolved fluorescence bioassay. J Fluoresc 15:559–568
16. Yuan J, Wang G (2006) Lanthanide-based luminescence probes and time-resolved luminescence bioassays. Trends Anal Chem 25:490–500
17. Reany O, Gunnlaugsson T, Parker D (2000) Selective signalling of zinc ions by modulation of terbium luminescence. Chem Commun 473–474

18. Hanaoka K, Kikuchi K, Kojima H, Urano Y, Higuchi T, Nagano T (2003) Selective detection of zinc ions with novel luminescent lanthanide probes. Angew Chem Int Ed 42:2996–2999
19. Ye Z, Wang G, Chen J, Fu X, Zhang W, Yuan J (2010) Development of a novel terbium chelate-based luminescent chemosensor for time-resolved luminescence detection of intracellular Zn^{2+} ions. Biosens Bioelectron 26:1043–1048
20. Song C, Ye Z, Wang G, Yuan J, Guan Y (2010) A lanthanide complex-based ratiometric luminescent probe specific for peroxynitrite. Chem—Eur J 16:6464–6472
21. Xiao Y, Zhang R, Ye Z, Dai Z, An H, Yuan J (2012) Lanthanide complex-based luminescent probes for highly sensitive time-gated luminescence detection of hypochlorous acid. Anal Chem 84:10785–10792
22. Dai Z, Tian L, Ye Z, Song B, Zhang R, Yuan J (2013) A lanthanide complex-based ratiometric luminescence probe for time-gated luminescence detection of intracellular thiols. Anal Chem 85:11658–11664
23. Tsien RY (1981) A non-disruptive technique for loading calcium buffers and indicators into cells. Nature 290:527–528
24. Koide Y, Urano Y, Kenmoku S, Kojima H, Nagano T (2007) Design and synthesis of fluorescent probes for selective detection of highly reactive oxygen species in mitochondria of living cells. J Am Chem Soc 129:10324–10325
25. Xiao Y, Ye Z, Wang G, Yuan J (2012) A ratiometric luminescence probe for highly reactive oxygen species based on lanthanide complexes. Inorg Chem 51:2940–2946
26. Song B, Wang G, Tan M, Yuan J (2006) A europium(III) complex as an efficient singlet oxygen luminescence probe. J Am Chem Soc 128: 13442–13450
27. Mocak J, Bond AM, Mitchell S, Scollary G (1997) A statistical overview of standard (IUPAC and ACS) and new procedures for determining the limits of detection and quantification: Application to voltammetric and stripping techniques. Pure Appl Chem 69:297–328